

Iron oxide-based honeycomb catalysts for the dehydrogenation of ethylbenzene to styrene

William P. Addiego*, Wei Liu, Thorsten Boger

Corning Incorporated, Sullivan Park-DV-01-9, Corning, NY 14831, USA

Abstract

Corning has recently developed a novel extrusion method to make bulk transition metal oxide honeycomb catalysts. One area of effort has been iron oxide-based catalysts for the dehydrogenation of ethylbenzene to styrene, a major chemical process that yields worldwide 20 MM tons/yr. In industry, the monomer is synthesized mostly in radial-flow fixed-bed reactors. Because of the high cross-sectional area for flow and shallow depth of the catalyst bed in these reactors, low reactor pressure gradients are maintained that favors the yield and selectivity for styrene formation. However, the radial-flow design has inherent detractions, including inefficient use of reactor volume and large temperature gradients that decrease catalyst service life. The overall economics of the process can be improved with parallel-channel honeycomb catalysts and axial flow reactors. The simple axial flow design of honeycomb catalysts provides low-pressure drop, while making more efficient use of reactor volume, with better heat and mass transfer characteristics compared to a conventional radial packed bed. An important part of this concept is the ability to fabricate a wide family of dehydrogenation catalyst compositions into honeycombs with the requisite chemical, physical, mechanical, and catalytic properties for industrial use. The ethylbenzene dehydrogenation (EBD) honeycomb catalysts developed by Corning have compositions similar to those commonly used in industry and are prepared with the same catalyst and promoter precursors and with similar treatments.

However, to enable extrusion of catalyst precursors into honeycomb shapes, especially at cell densities above 100 cell/in.², Corning's process compensates for the high salt concentrations and the high pH of the batch material that would otherwise prevent or impede honeycomb extrusion. The improved rheological characteristics provide the necessary plasticity, lubricity, and resiliency for honeycomb extrusion with sufficient binder strength needed before calcination to the final product. Iron oxide-based honeycombs after calcination are strong and possess macroporosity and high surface area. In bench-scale testing, particular honeycomb catalyst compositions exhibited 60–76% ethylbenzene conversion with styrene selectivity of 95–91%, respectively, under conventional reaction conditions without apparent deactivation or loss of mechanical integrity.

© 2001 Elsevier Science B.V. All rights reserved.

Keywords: Iron oxide; Honeycomb; Catalysts; Dehydrogenation; Ethylbenzene; Styrene; Axial flow; Reactor

1. Introduction

The industrial process for the dehydrogenation of ethylbenzene to styrene is used to make valuable commodity chemicals such as polystyrene and synthetic rubber such as ABS and SB latex; as much as 20 MM

tons/yr of styrene monomer are made. Although this process was already commercialized in the 1930s, research and development has continued to improve it, including the development of new catalysts, reactor designs and process routes [1–13].

The non-oxidative ethylbenzene dehydrogenation (EBD) to styrene is endothermic, reversible and equilibrium limited. Because of the thermodynamic limitation, the formation of styrene is favored by the

* Corresponding author. Fax: +1-607-974-3745.

E-mail address: addiegowp@corning.com (W.P. Addiego).

low partial pressure of ethylbenzene and hydrogen. To promote the forward reaction, the industrial process uses steam, where the molar ratio of steam to ethylbenzene is 6–13:1 at atmospheric or vacuum conditions. Steam provides heat for the reaction, prevents over-reduction of the iron oxide-based catalyst, prevents coke formation, and decreases the partial pressure of gases, thereby shifting the chemical equilibrium to higher styrene conversion [3,13].

For low reactor pressure drop, industrial EBD is performed in radial-flow reactors, as shown in Fig. 1(a). Total ethylbenzene conversion through both reactors is about 60–70%. An axial flow honeycomb reactor, shown in Fig. 1(b), could improve overall efficiency by incorporating heat exchangers to minimize thermal gradients along the catalyst bed, improving the performance and extending the service life of the

Table 1

Pressure drop comparison of honeycomb and packed bead with equivalent bed cross-section

Bed properties	Honeycomb		Bead
Void fraction	0.5		
Linear velocity (m/s)	6.8		
Wall thickness (mm)	1	0.5	3.2 ϕ
Cell density (cpsi)	55	220	N/A
Pressure drop (bar/m)	0.021	0.085	0.437
Characteristic heat/mass transfer dimension (mm)	0.5	0.25	0.8

catalyst, while maintaining low-pressure drop [14]. With a higher geometric surface area relative to packed beads, the honeycomb also has a better mass/heat transfer dimension, as shown in Table 1.

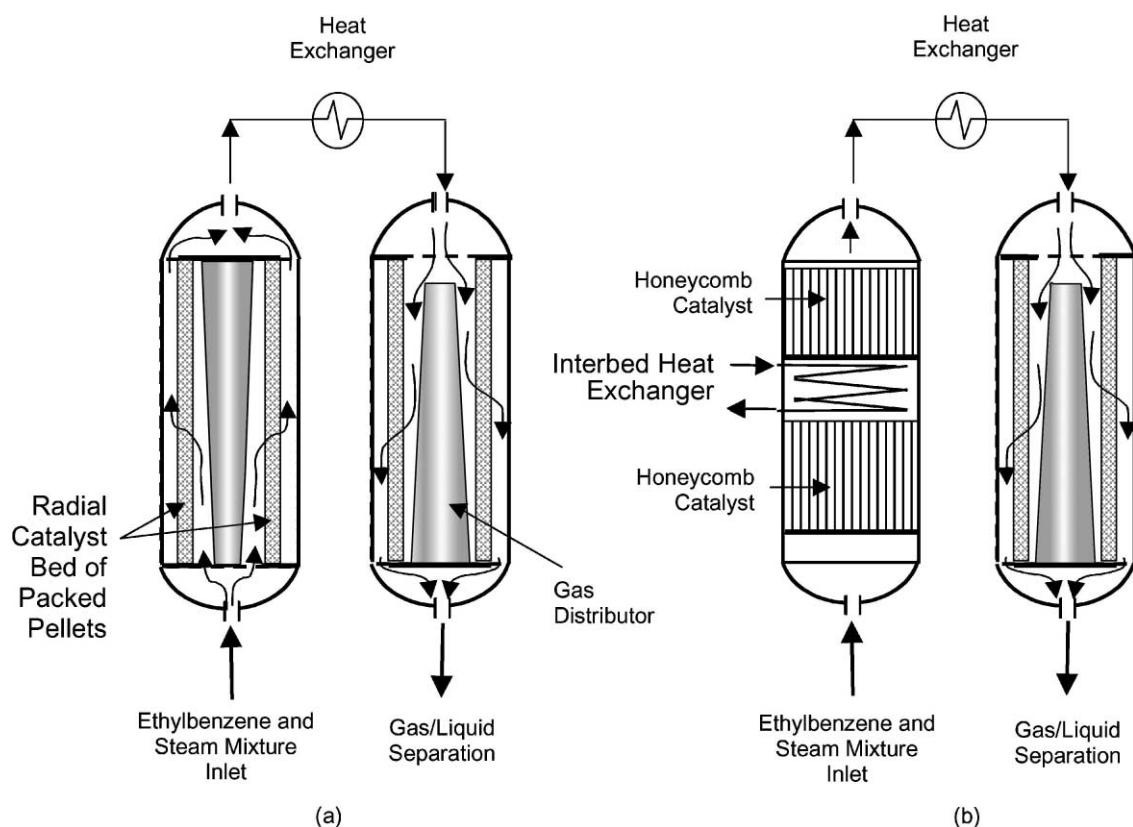


Fig. 1. (a) Diagram of a first-stage radial-flow reactor with cylindrical shaped packed catalyst bed held in place by concentric screens and with a central conical gas distributor. (b) Axial flow honeycomb catalyst reactor with interbed heat exchanger. In both configurations, effluent is sent to a second-stage reactor to dehydrogenate remaining ethylbenzene.

Industrial dehydrogenation compositions are a complex mixture of metal oxides and large amounts of salts, principally iron oxide and potassium carbonate. During reaction start-up, under essentially reduction conditions, the catalytically active potassium ferrite, KFeO_2 , forms along with ferrite polymorphs [16,20–22]. In addition, potassium carbonate also acts as a catalyst to oxidize carbonaceous deposits to prevent coking [3]. The literature is replete with studies on EBD catalysts [2–6,13,15–24].

Controlling the rheological properties of the catalyst compositions is important in order to provide the requisite plasticity and lubricity during extrusion needed for web formation and knitting, skin formation, and stiffening as the honeycomb emerges from the die. However, because of the large concentration of salts in typical dehydrogenation catalyst compositions, extrusion rheology is usually degraded with the loss of plasticity and water migration. This occurs, in part, because salts can induce the precipitation of organics and the loss of “bound” water layers associated with organics and distributed throughout the extrusion batch. The proper combination of organic additives and materials processing is necessary to extrude honeycomb catalysts containing high salt concentration and avoid or attenuate adverse ionic shock. This paper reports on a method of extruding industrial-type EBD catalysts, their characterization and catalytic performance.

2. Experimental

2.1. Extrusion compositions

Extrusion batches were made in a manner similar to industrial methods. $\alpha\text{-Fe}_2\text{O}_3$ was mixed with

appropriate amounts of K_2CO_3 , $(\text{NH}_4)_6\text{Mo}_7\text{O}_{24}$, CeCO_3 , and MgCO_3 or CaCO_3 , based on the analyzed equivalent oxide of the salts, as listed in Table 2. The catalyst precursors were dry-blended in a tubular mixer with certain organic additives. After dry blending, organic emulsions were added with water, along with additional plasticizers and lubricants, and milled to form a plastic dough, that was subsequently homogenized to ensure a thorough mixing of solid and liquid components. Honeycombs were then extruded with square cells of 100, 200, and 400 cell/in.² (cpsi) with web thickness of 0.64, 0.38, and 0.18 mm, respectively. Extrusion rheology was measured with a parallel-plate rheometer.

2.2. Chemical and physical characterization and catalyst testing

After extrusion, honeycombs were dried at 80°C and calcined at 850°C/6 h. Calcined samples of 100 cpsi honeycombs were characterized for surface area, porosity, pore size distribution, A-axis crushing strength, and catalytic activity and selectivity for styrene formation. As shown in Table 3, honeycomb catalysts which had a BET surface area of 4 m²/g were macroporous with >50% porosity. Honeycombs were very strong, exhibiting an A-axis crushing strength (i.e., force applied parallel to cell walls) of 1300–2000 psi after calcination.

Honeycomb catalysts were also tested for catalytic performance using an integral reactor. The reactor consisted of a stainless steel tube within which a 1-in. diameter quartz tube was inserted to support a 50 cm³ honeycomb catalyst, 2.5 cm (ID) \times 10.0 cm long. –60 mesh SiC particles were packed above and below the honeycomb, separated from the honeycomb by quartz

Table 2
EBD catalyst compositions

Component	Batch component	Oxide (wt.%)	Function/promoter	Compositions oxide (wt.%)	
				J-A, 2J-AB	Q-B1
Fe_2O_3	Oxide	25–80	Activity	72	79
K_2O	Carbonate	10–35	Activity	16	11
CeO_2	Carbonate	0–5	Activity	4	4
MoO_3	Ammonium molybdate	0–3	Selectivity	1	3
CaO	Carbonate	0–3	Chemical/mechanical stability	0	2
MgO	Carbonate	0–10	Chemical/mechanical stability	7	1

Table 3

Physical and mechanical characteristics of 100 cpsi EBD honeycomb catalysts calcined at 850°C/6 h

Honeycomb catalyst	Surface area (m ² /g)	A-axis compression strength (psi)	Apparent density (g/ml)	% Porosity	Median pore size (nm)
J-A	4.0	1300	3.9	53	350
Q-B1	3.0	1800	4.4	56	380
2J-AB	3.5	2000	3.9	54	330

wool. Thermocouples were placed at the honeycomb entrance and exit in the SiC packing for uniform temperature measurement. Above the SiC packing, dense α -alumina beads were packed to help the heat feed uniformly before entering the honeycomb.

Reagent grade ethylbenzene and de-ionized water were delivered to the top of the reactor by two liquid pumps in order to provide the appropriate steam to ethylbenzene ratio. The mixture was vaporized in the reactor as it flowed to the honeycomb catalyst. The effluent was cooled and liquid product and gas were then separated. Hydrocarbons were separated from water and measured by gas chromatography.

3. Results and discussion

3.1. Extrusion behavior

Extrusion compositions were prepared with various polymer emulsions to affect rheology. For this part of the study, one particular inorganic composition was used, J-A listed in Table 2. These were compared to extrusion performance without organics or with soluble cellulose ethers. Certain polymer emulsions were suitable for extruding honeycombs and superior to water-soluble organic extrusion aids, providing plasticity to an extent that honeycomb matrix formation was possible with a 100 cpsi/0.7 mm geometry or greater. Systems with appropriate colloidal polymer emulsions set and dried rapidly without cracking and showed considerable green strength before calcination.

The impact of polymer glass transition temperature, T_g , on extrusion rheology was measured, based on changes in the batch material's stiffness or rigidity as a function of the complex modulus, G^* . Extrusion batches containing a soft polymer with a T_g near or below ambient stiffened much more rapidly during processing at ambient temperatures than batches

containing glassy polymers with a T_g significantly above the mixing or extrusion temperature, as shown in Table 4. The elastic modulus, G' , of a batch containing a glassy polymer increased rapidly after 1 h, as shown in Fig. 2, due to polymer cross-linking at the typically high batch pH ≈ 9 , rendering the batch brittle and less capable of plastic deformation. With the appropriate organic system, the batch remained sufficiently plastic during extrusion. Honeycombs rapidly set at temperatures near the T_g of the polymer and dried with little or no cracking. This feature minimized distortion of the honeycomb matrix.

Water-soluble extrusion aids, such as cellulose ethers and polyethylene oxides, are very susceptible to ionic shock and tend to precipitate in the presence of fairly low concentrations of alkali salts, especially carbonate and sulfate salts [25,26]. In extrusion batches containing K_2CO_3 , these polymers easily flocculate, lose the ability to disperse water, and contribute to the overall degradation of extrusion rheology. The yield stress of extrusion batches with different types of organic systems was approximated from the G^* modulus at a shear frequency of 1 rad/s and 5% strain and is listed in Table 5. The amount of liquid to plasticize the batch was normalized to a reference batch not containing any organic additive. A significant amount of water was needed to plasticize the reference, which showed a low yield stress of 19 kPa. Less water was required after adding methylcellulose, raising the yield stress, but honeycombs

Table 4

Effect of organic additive T_g on setting time of EBD catalyst extrusion batch

Polymer emulsion	T_g (°C)	Setting time (min)	Complex modulus (kPa)
EM101	<0	30	>350
VM501	<15	90	>350
RT502	>75	140	>350

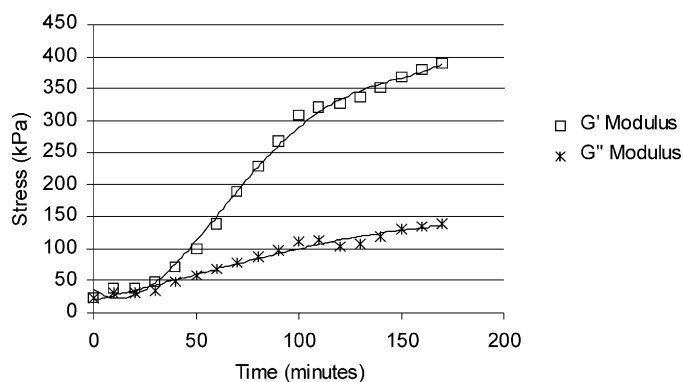


Fig. 2. The elastic modulus, G' , increases more rapidly during processing than the viscous modulus, G'' , as the organic binder sets, stiffening the extrudate. The high salt concentration and pH of the extrusion batch promotes binder setting.

Table 5
Effect of organic additives on yield stress of EBD catalyst extrusion batch

Organic additives	Extrusion quality	Yield stress (kPa)	% Liquid ^a
No organic	Matrix collapse soft, tearing	19	100
Methylcellulose	Matrix distortion slumping	31	46
Organic pack 1	Matrix collapse slumping	9	69
Organic pack 2	No matrix distortion	61	57

^a The amount of water and aqueous emulsion in the batch and normalized to the liquid content of the composition containing no organic additives.

were easily deformed. After drying and calcination, the material was brittle and weak. Another extrusion batch exhibited a very low yield stress because of the relatively high concentration of polymer emulsion in the batch. Lowering the emulsion concentration and decreasing the water content raised the yield stress to 61 kPa with sufficient stiffness under shear to extrude a plastic material into honeycombs with little or no matrix distortion. As shown in Fig. 3, an extrusion using organic pack 2 had a significantly higher G^* than all of the other extrusion batches. Consequently, honeycombs were more resilient emerging from the extrusion die than honeycombs of the other softer compositions. Examples of the extrudates that had a high yield stress are shown in Fig. 4 with cell densities up to 400 cpsi.

3.2. Catalytic performance

The J-A honeycomb catalyst was tested and compared with the literature, as shown in Table 6. As

expected, the ethylbenzene conversion increased with an increase in the steam/EB ratio and decreased when the bed temperature was lowered. Selectivity toward styrene decreased with higher EB conversion and increased with low steam/EB ratio and bed temperature. Although not shown, ethylbenzene conversion decreased with an increase in the space velocity, as expected. In addition, the major by-products were benzene and toluene, and phenylacetylene concentration was less than 200 ppm. Styrene selectivity was as high as 93% with an EB conversion of 67% at a low steam/EB ratio. Fig. 5 shows the selectivity and yield as a function of EB conversion. The model was calculated by determining a best-fit equation from experimental data. Experimental data fit well with that reported in the literature [2,7–9].

During the reaction, catalyst surface area decreased to about 2 m²/g and porosity decreased to 45–50%. These changes were associated with the formation of potassium ferrites under reducing conditions. While no catalytic deactivation was observed during the

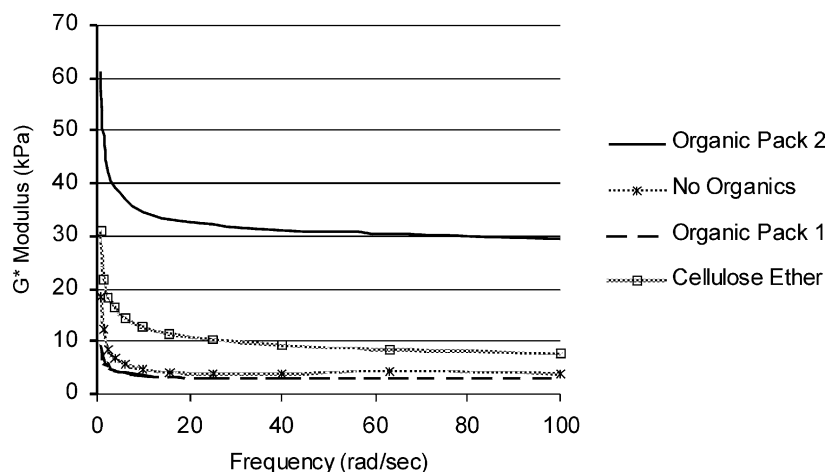


Fig. 3. The G^* modulus measures the rigidity of the batch material. Initially, shear-thinning lowers G^* as the shear rate (frequency) increases. The lower the G^* , the softer the material. G^* is affected by the type and concentration of organic additives in the extrusion batch.

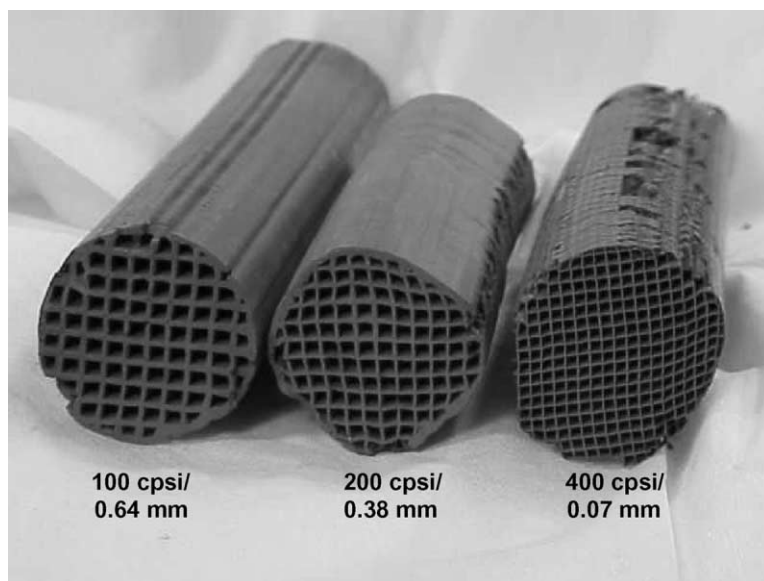


Fig. 4. Extruded EBD honeycomb catalysts.

Table 6
Catalytic performance of EBD honeycomb catalysts

	J-A honeycomb catalysts				Literature values ^a	
T ($^{\circ}\text{C}$)	609	605	588	584	593	593
$\text{H}_2\text{O}/\text{EB}$ molar ratio	13.4	6.7	13.4	13.4	12.2	9.3
LHSV	0.48	0.48	0.48	0.48	0.48	0.48
Conversion (%)	76.3	66.7	68.2	59.5	68.1	64.8
Selectivity (%)	90.7	93.3	93.4	95.2	92.4	92.3

^a Ref. [8].

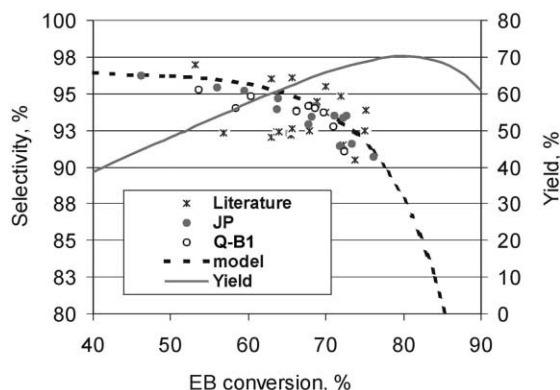


Fig. 5. Selectivity and yield for styrene as a function of ethylbenzene conversion during dehydrogenation. Comparison of honeycomb catalysts with literature values [2,7–9].

reaction, formation of catalytically inactive magnetite and potassium hydroxide might have also occurred to some extent [22].

4. Summary and conclusions

Highly active and selective industrial-type EBD catalysts were extruded into strong honeycombs. With the proper polymer emulsion and concentration, there was sufficient plasticity and lubricity for extruding compositions with high concentrations of potassium carbonate and a high pH. The yield stress was high enough for the honeycomb matrix to support itself with cell densities up to 400 cpsi without slumping or distortion. Processing time was extended by using a polymer with a T_g significantly above ambient. Honeycombs were rapidly set by drying the honeycomb near the T_g of the polymer, minimizing distortions as the honeycomb dried. Calcined honeycomb catalysts were strong, with crushing strengths from 1300 to 2000 psi. The honeycombs were generally macroporous with >50% porosity.

Catalytic performance was generally equivalent to packed beads reported in the literature. Styrene selectivity was 95–91% with 60–76% EB conversion.

The results have shown that dehydrogenation catalysts with a complex set of precursors can be

extruded into honeycombs of various cell geometries with proper rheological control. The honeycomb is converted into an active catalyst under reaction conditions, while retaining its structure without loss of mechanical integrity.

References

- [1] A.A. Savoretti, D.O. Borio, V. Bucala, J.A. Porras, *Chem. Eng. Sci.* 54 (1999) 205–213.
- [2] Q. Chen, X. Chen, L. Mao, W. Cheng, *Catal. Today* 51 (1999) 141–146.
- [3] F. Cavani, F. Trifiro, *Appl. Catal.* 133 (1995) 219–239.
- [4] G. Kolios, G. Eigenberger, *Chem. Eng. Sci.* 54 (1999) 219–239.
- [5] N. Mimura, M. Saito, *Catal. Today* 55 (2000) 173–178.
- [6] N. Mimura, I. Takahara, M. Saito, T. Hattori, K. Ohkuma, M. Ando, *Catal. Today* 45 (1998) 61–64.
- [7] H.-J. Kremer, US 5 097 091.
- [8] D.K. Kim, G.M. Longland Jr., US 5 503 572 (1991).
- [9] D.L. Williams, K.J. Russ, E.K. Dienes, G.A. Laufer, US 5 023 225 (1991).
- [10] C.-C. Chu, US 4 503 163 (1985).
- [11] J.T. Smith, B.S. Masters, D.J. Smith, US 4 467 046 (1984).
- [12] P.W. Dellinger, R.G. Moore, F.A. Sherrod, A.R. Smith, US 5 510 552 (1996).
- [13] E.H. Lee, *Catal. Rev.* 8 (2) (1973) 285–305.
- [14] T. Boger, W. Liu, W.P. Addiego, S.A. Campbell, (2001), 6th World Congress to Chemical Engineering.
- [15] T. Hirano, *Appl. Catal.* 26 (1986) 65–79.
- [16] T. Hirano, *Appl. Catal.* 26 (1986) 81–90.
- [17] T. Hirano, *Appl. Catal.* 26 (1986) 119–132.
- [18] V.K. Kaushik, T.S.R.P. Rao, B.L.S. Yadav, M.S. Chhabra, *Appl. Surf. Sci.* 32 (1988) 93–98.
- [19] G.E. Vrieland, P.G. Menon, *Appl. Catal.* 77 (1991) 1–8.
- [20] W. Weiss, D. Zscherpel, R. Schlögl, *Catal. Lett.* 52 (1998) 215–220.
- [21] A. Trovarelli, C. deLeitenburg, M. Boaro, G. Dolcetti, *Catal. Today* 50 (1999) 353–367.
- [22] M. Muhler, R. Schlögl, A. Reller, G. Ertl, *Catal. Lett.* 2 (1989) 201–210.
- [23] N.J. Jebarathinam, N.J.M. Eswaramoorthy, V. Krishnasamy, *Appl. Catal. A* 145 (1996) 57–74.
- [24] W.P. Addiego, C.A. Estrada, D.W. Goodman, M.P. Rosynek, R.G. Windham, *J. Catal.* 146 (2) (1994) 407–414.
- [25] Methocel™ Cellulose Ethers Technical Handbook, The Dow Chemical Company, 1997.
- [26] F.W. Stone, J.J. Stratta, in: H.F. Mark, N.G. Gaylord, N.M. Bikales (Eds.), *Encyclopedia of Polymer Science and Technology*, Vol. 6, Wiley, New York, 1967, pp. 103–145.